Journal of Applied Biomedicine 16 (2018) 328–336

Contents lists available at ScienceDirect

Journal of Applied Biomedicine

journal homepage: www.elsevier.com/locate/jab

Original research article

A proteomic glimpse into the oncogenesis of prostate cancer

Patrícia Borba Martiny[a,*], Diego Duarte Alcoba[a], Brasil Silva Neto[b], Paulo Costa Carvalho[c], Ilma Simoni Brum[a]

[a] Universidade Federal do Rio Grande do Sul, Institute of Health Sciences, Department of Physiology, Porto Alegre, Brazil
[b] Hospital de Clínicas de Porto Alegre, Service of Urology, Porto Alegre, Brazil
[c] Carlos Chagas Institute, Laboratory of Proteomics and Protein Engineering, Fiocruz, Paraná, Brazil

ARTICLE INFO

Article history:
Received 7 June 2017
Received in revised form 24 April 2018
Accepted 16 May 2018
Available online 24 May 2018

Keywords:
Prostate cancer
Benign prostatic hyperplasia
Proteomics
Tandem mass tag
Mass spectrometry

ABSTRACT

Prostate cancer (PCa) is the second most frequent cancer in men worldwide. Distinguishing between the nonaggressive and aggressive forms of this disease is difficult, and a means to better characterize molecular patterns that could aid in diagnosis is urgently needed. Here, we compare the proteomic profiles of PCa and benign prostatic hyperplasia (BPH) in an effort to elucidate underlying mechanisms of oncogenesis. We compared protein expression in PCa and BPH tissue biopsies using quantitative tandem mass tag (TMT) and a MultiNotch data acquisition proteomic on an Orbitrap Fusion. Four proteins that were observed to be differentially abundant in the mass spectrometry analysis were selected for further comparison with quantitative real-time PCR: S100A4, L-lactate dehydrogenase B-chain (LDHB), Phosphatidylethanolamine-binding-protein 1-RAF (RKIP), and Ras suppressor-protein-1 (RSU1). Mass spectrometry showed RKIP and RSU1 to be upregulated in PCa, while S100A4 and LDHB were upregulated in BPH. q-PCR results were in agreement with quantitative proteomic data in BPH tissue but disagree with gene expression analysis of PCa samples. These four elements showed higher gene expression in BPH than in PCa. Taken together, our results complement and reinforce the current understanding of prostate cancer progression.

Introduction

Prostate cancer (PCa) is a heterogeneous disease and is the most common noncutaneous solid tumor in men worldwide (Jemal et al., 2010). It is expected that in the US alone over 164,000 men will be diagnosed with PCa in 2018, causing over 29,000 deaths (Siegel et al., 2018). In addition, benign prostatic hyperplasia (BPH) is one of the most common benign diseases among all men and, as with PCa, the incidence of BPH increases with age. PCa is a relatively slow progressing and indolent disease, and it is typically treated surgically when the disease remains localized. Following surgery patients are usually treated with anti-androgen therapies. However, when PCa recurs after anti-androgen treatment, it can become more aggressive, unresponsive to treatment, and more prone to metastasize. PCa has a high rate of recurrence, with more than 40% of patients who undergo primary curative therapy experiencing disease progression (Kozal et al., 2015).

The most widely adopted method to diagnose benign or malignant growth of the prostate is to check for elevated serum prostate-specific antigen (PSA); however, PSA test sensitivity and specificity is considered unsatisfactory for accurate diagnosis (Bayat et al., 2015; Charrier et al., 2001; Garbis et al., 2008) and is useless for the 15% of PCa cases that occur in men with normal PSA serum levels (De Marzo et al., 1999). The overlap of symptoms in BPH and prostate cancer, along with the lack of discrimination between these two prostate diseases by PSA, presents a diagnostic dilemma that clinicians face when dealing with prostate disease (Bayat et al., 2015; Jedinak et al., 2015; Mazzucchelli et al., 2000).

BPH comprises a prostate overgrowth with rare genetic abnormalities; it is expected that many of the differences that can be observed between BPH and cancerous epithelia will reflect this particular aspect of prostate tumor biology (De Marzo et al., 1999).

PCa protein expression analysis is a valuable strategy for understanding physiopathological mechanisms related to prostate disease. Recent advances in the field of proteomics have enabled detailed analysis of complex protein mixtures (Pin et al., 2013). The

* Author for correspondence: Universidade Federal do Rio Grande do Sul, Institute of Health Sciences, Department of Physiology, Sarmento Leite Street, 500, Porto Alegre, Brazil.
E-mail address: patricia.martiny@ufrgs.br (P.B. Martiny).

https://doi.org/10.1016/j.jab.2018.05.003
1214-021X/

ability to analyze proteomes directly has been a critical technological development since proteins are responsible for the phenotypes of cells, and elucidating mechanisms of diseases solely by studying their genome is not sufficient. Therefore, studies that can pinpoint proteins involved in a heterogenic disease, such as PCa and BPH, may help the clinicians to discriminate these two prostate diseases and provide a better understanding, at the molecular level, of this pathology.

There has been also an increasing interest in applying proteomics to assist in understanding the pathogenesis of PCa, elucidating the mechanism of drug resistance and developing biomarkers for early detection (Garbis et al., 2008; Jedinak et al., 2015; Whitfield et al., 2006; Zeidan et al., 2015). Many of the molecular mechanisms underlying the complex clinical findings of prostate disease remain unknown, highlighting the need for advances in biomedical research to unravel novel molecular discoveries in prostate and other cancers.

This report compares the gene and protein expression of BPH *versus* PCa prostate tissue specimens. Our quantitative proteomic approach employed Tandem Mass Tags (Thompson et al., 2003) and a MultiNotch single shot approach (McAlister et al., 2014; Washburn et al., 2001). Four differentially abundant proteins of interest were further validated by quantitative real-time RT-PCR (qPCR).

Materials and methods

Patients and specimens

The Ethical Review Board from *Hospital de Clinicas de Porto Alegre* approved this study under license number 110283. Written informed consent to provide tissue samples for scientific purposes was obtained from all six patients who underwent radical prostatectomy surgery at the Urological Service from *Hospital de Clinicas of Porto Alegre*. PCa and BPH tissues were obtained during a radical prostatectomy surgery. The prostate was macroscopically evaluated by a urologist and an experienced pathologist immediately after the surgery to confirm the anatomopathological diagnosis.

Histopathological characterization was performed using hematoxylin-eosin stained sections of formalin fixed and paraffin embedded specimens. Tumors were classified using the Gleason grading system. Gleason grading is accepted as the international standard for pathological grading in prostate cancer, and grades vary from 2 to 10. Gleason scores are calculated by adding the grade of the two more abundant patterns observed in each specimen (Gleason, 1992).

Protein preparation

Proteins were extracted from three prostate carcinoma and three benign prostate hyperplasia samples. 100 μg of total protein from each sample were denatured, cysteine blocked, and digested with trypsin for 18 h as described in the standard protocol of Tandem Mass Tag™ sixplex (Thermo Scientific™). The TMT™ Reagents Kit was from Life Technology (USA). The trypsin was from Promega, 224 (Madison, Wisconsin, USA). Acetonitrile, isopropanol, acetone, formic acid, glycerol, sodium citrate buffer were from Sigma-Aldrich (USA). KCl, KH_2PO_4, NaCl, Tris, EDTA, Triton X-100, SDS were from Invitrogen (Carlsbad, CA, USA).

PCa samples were labeled with TMT™ tags 126, 127, and 128; BPH samples were labeled with 129, 130 and 131. Analysis was performed using a Thermo EASY-nLC chromatography system coupled online with an Orbitrap Fusion (Thermo, San Jose) through an in-house built electrospray stage. Data were acquired using the MultiNotch MS3 method (McAlister et al., 2014), with scan range of 400–1600 *m/z*, a resolution of 120,000 for survey scans, an AGC target of 500,000 (FTMS1). All. raw files from mass spectrometer are accessible at http://proteomics.fiocruz.br/supplementaryfiles/pmartiny2016/.

RNA isolation and real time PCR (qPCR)

Protein abundance of the differentially abundant proteins was correlated with mRNA expression levels using a 96-well Custom TaqMan® Array Plates (#4413257 catalog number #PP5OQI1 assay ID) preloaded with 4 selected genes (Table 1). These genes were chosen based on their differential abundance magnitude as determined by our proteomic results. Total RNA was extracted from PCa, BPH and non-neoplastic prostate tissues using Trizol (Invitrogen, Carlsbad, CA, USA), and transcribed to cDNA using Superscript III Reverse Transcriptase (Invitrogen, Carlsbad, CA, USA), according to manufacturer's instructions. For each gene of interest, we performed experimental duplicates and the expression levels were normalized to the average expression of the *housekeeping* gene B2M (Hs99999907_m1). For the quantitative RT-qPCR assays, 1 ng cDNA/well was used and the reactions were performed using gene-specific double fluorescent labeled TaqMan® in a fast RT-qPCR system (Applied Bio-systems StepOnePlus™ Real-Time PCR System). The reaction was initiated at 50 °C for 2 min, 95 °C for 20 s, 40 cycles at 95 °C for 1 s and 60 °C for 20 s, according TaqMan® Fast Advanced Master Mix manufacturer's instructions. The relative mRNA expression level was determined using the widely used $2^{\Delta\Delta Ct}$ analysis method. For the relative expression analysis of PCa and BPH, the expression level of control non-neoplastic prostate samples was used as calibrator.

Data analysis

The reference proteome set of *Homo sapiens* was downloaded from the UniProt consortium on January 21st, 2015. PatternLab (Carvalho et al., 2016) was used to generate a target-decoy database by grouping subset sequences, adding the sequences of 127 common mass spectrometry contaminants, and by including a reversed version of each sequence. The final database used for peptide sequence matching contained 138,196 sequences.

Peptide spectrum matching and quality assessment

The Comet 2015 rev. 2 search engine, which is embedded into PatternLab for proteomics 4.0 (Carvalho et al., 2016), was used to compare experimental tandem mass spectra against those theoretically generated from our sequence database and to select the most likely peptide sequence candidate for each spectrum. The

Table 1
Gene and protein accession to NCBI and swissprot.

Gene accession number	Protein accession number	Name of the protein	Gene symbol
NM 002952.1	P26447	S100 calcium binding protein A4	S100A4
NM 001174097.1	P07195	L-lactate dehydrogenase B	LDHB
NM 002567.2	P030086	Phophatidylethanolamine-binding protein 1 RAF	PEBP1
NM 012425.3	Q15404	Ras supressor protein 1	RSU1

Table 2
Seventy-seven differentially abundant proteins up and down regulated on PCa.

ID Protein	Symbol	Protein	Absolut fold change	Upregulation in PCa	Downregutation in PCa
P05109	S100A8	Protein S100-A8	7.1295*		↓
P06702	S100A9	Protein S100-A9	6.1790*		↓
Q08380	LGALS3BP	Galectin-3-binding protein	4.2585*		↓
P26447	S100A4	Protein S100-A4	3.9152*		↓
P25311	AZGP1	Zinc-alpha-2-glycoprotein	3.1605*		↓
P02511	CRYAB	Alpha-crystallin B chain	2.8001*		↓
P78417	GSTO1	Glutathione S-transferase omega-1	2.5744*		↓
P01011	SERPINA3	Alpha-1-antichymotrypsin	2.4982*		↓
P06703	S100A6	Protein S100-A6	2.3668*		↓
P31947	SFN	14-3-3 protein sigma	2.0574*		↓
Q05707	COL14A1	Collagen alpha-1(XIV) chain	1.9551*		↓
P04083	ANXA1	Annexin A1	1.9087*		↓
P35579	MYH9	Myosin-9	1.8029*		↓
J9JID7	LMNB2	Lamin B2, isoform CRA_a	1.6978*		↓
O14558	HSPB6	Heat shock protein beta-6	1.6492*		↓
P07355-2	ANXA2	Isoform 2 of Annexin A2	1.6427*		↓
P24844	MYL9	Myosin regulatory light polypeptide 9	1.5178*		↓
P49189	ALDH9A1	4-trimethylaminobutyraldehyde dehydrogenase	1.5148*		↓
P19338	NCL	Nucleolin	1.4833*		↓
Q99497	PARK7	Protein DJ-1	1.4408*		↓
P07288	KLK3	Prostate-specific antigen	1.4038*		↓
P37802-2	TAGLN2	Isoform 2 of Transgelin-2 OS=Homo sapiens	1.3774*		↓
P07195	LDHB	L-lactate dehydrogenase B chain	1.3733*		↓
P08670	VIM	Vimentin	1.3719*		↓
O94760	DDAH1	N(G),N(G)-dimethylarginine dimethylaminohydrolase 1	1.3596*		↓
O75874	IDH1	Isocitrate dehydrogenase [NADP] cytoplasmic	1.3461*		↓
P08133	ANXA6	Annexin A6	1.3434*		↓
P67936	TPM4	Tropomyosin alpha-4 chain	1.3287*		↓
P17661	DES	Desmin	1.3154*		↓
Q9Y490	TLN1	Talin-1	1.3102*		↓
P09382	LGALS1	Galectin-1	1.3036*		↓
P30101	PDIA3	Protein disulfide-isomerase A3	1.2997*		↓
Q8NBS9	TXNDC5	Thioredoxin domain-containing protein 5	1.2971*		↓
P00441	SOD1	Superoxide dismutase [Cu-Zn]	1.2907*		↓
P09211	GSTP1	Glutathione S-transferase P	1.2804*		↓
P10809	HSPD1	60 kDa heat shock protein, mitochondrial	1.2626*		↓
P04792	HSPB1	Heat shock protein beta-1	1.2550*		↓
Q01518	CAP1	Adenylyl cyclase-associated protein 1	1.2462*		↓
P62491	RAB11A	Ras-related protein Rab-11A	1.2388*		↓
P30041	PRDX6	Peroxiredoxin-6	1.2046*		↓
P04179	SOD2	Superoxide dismutase [Mn], mitochondrial	1.1950*		↓
P07585	DCN	Decorin	1.1819*		↓
P23284	PPIB	Peptidyl-prolyl cis-trans isomerase B	1.1666*		↓
P08758	ANXA5	Annexin A5	1.1631*		↓
P62937	PPIA	Peptidyl-prolyl cis-trans isomerase A	1.1643#	↑	
Q9NR45	NANS	Sialic acid synthase	1.1783#	↑	
P30086	PEBP1	Phosphatidylethanolamine-binding protein 1-RAF	1.2010#	↑	
P01009	SERPINA	Alpha-1-antitrypsin	1.2142#	↑	
P02787	TF	Serotransferrin	1.2363#	↑	
P62805	HIST1H4A	Histone H4	1.2664#	↑	
P08107	HSPA1A	Heat shock 70 kDa protein 1A/1B	1.2676#	↑	
P27797	CALR	Calreticulin	1.2727#	↑	
P07737	PFN1	Profilin-1	1.3010#	↑	
P00338-3	LDHA	Isoform 3 of L-lactate dehydrogenase A	1.3050#	↑	
J3KNQ4	PARVA	Alpha-parvin	1.3287#	↑	
P20774	OGN	Mimecan	1.3353#	↑	
P06396	GSN	Gelsolin	1.3542#	↑	
Q01995	TAGLN	Transgelin	1.3596#	↑	
P06733	ENO1	Alpha-enolase	1.3705#	↑	
Q15404	RSU1	Ras suppressor protein 1	1.4641#	↑	
P04406	GAPDH	Glyceraldehyde-3-phosphate dehydrogenase	1.4729#	↑	
P02790	HPX	Hemopexin	1.5148#	↑	
P02768	ALB	Serum albumin	1.6328#	↑	
P01861	IGHG4	Ig gamma-4 chain C region	1.6843#	↑	
P10768	ESD	S-formylglutathione hydrolase	1.8652#	↑	
P01859	IGHG2	Ig gamma-2 chain C region	1.8935#	↑	
P02647	APOA1	Apolipoprotein A-I	2.0207#	↑	
P21810	BGN	Biglycan	2.3386#	↑	
P68871	HBB	Hemoglobin subunit beta	3.8723#	↑	
P69905	HBA1	Hemoglobin subunit alpha	4.0103#	↑	
P02743	APCS	Serum amyloid P-component	4.5996#	↑	
P08729	KRT7	Keratin, type II cytoskeletal 7	5.1554#	↑	

Table 2 (*Continued*)

ID Protein	Symbol	Protein	Absolut fold change	Upregulation in PCa	Downregutation in PCa
Q15149	PLEC	Plectin	0.7195[#]	↑	
P23526	AHCY	Adenosylhomocysteinase	0.7074[#]	↑	
P21796	VDAC1	Voltage-dependent anion-selective channel protein 1	0.7231[#]	↑	
O75368	SH3BGRL	SH3 domain-binding glutamic acid-rich-like protein	1.2512[#]	↑	
P20674	COX5A	Cytochrome c oxidase subunit 5A, mitochondrial	0.8170[#]	↑	

[*] Values of BPH when compared with PCa.
[#] Values of PCa when compared with BPH.

search was limited to fully-tryptic peptide candidates; we imposed carbamidomethylation of cysteine and the modifications of the TMT reagents as fixed. The search engine accepted peptide candidates within a 40-ppm tolerance from the measured precursor *m/z,* up to two missed-cleavages, and used the XCorr as the primary search engine score.

PSM validity was assessed using the search engine processor (SEPro) that is embedded in PatternLab. Identifications were grouped by charge state (+2 and > +3), resulting in two distinct subgroups. For each result, the Comet XCorr, DeltaCN, DeltaPPM, and Peaks Matched values were used to generate a Bayesian discriminator. The identifications were sorted in non-decreasing order according to the discriminator score. A cutoff score was established to accept a false-discovery rate (FDR) of 1% at the peptide level based on the number of labeled decoys. This procedure was independently performed on each data subset, resulting in an FDR that was independent of charge state. Additionally, a minimum sequence length of six amino-acid residues was required. Results were post-processed to only accept PSMs with less than 6 ppm from the global identification average. "One-hit wonders" (*i.e.*, proteins identified with only one mass spectrum) having an XCorr of less than 2.5 were discarded. This last filter led to protein level FDRs below 1% for all search results.

Pinpointing differentially abundant proteins

Using TMT reporter ion signals, we statistically pinpointed proteins that changed in abundance by following the method described in a published bioinformatics protocol (Thompson et al., 2003). Briefly, PatternLab's isobaric analyzer module begins by linking the corresponding MultiNotch MS3 data with each respective tandem mass spectrum. Isotopic impurity corrections are carried out using the correction factors provided in the TMT kit. Then normalization for each channel is carried out according to each respective Total Ion Current. In what follows, the software performs a paired-peptide-centric statistical approach to assign p-values for each peptide as being differentially abundant or not. These individual p-values are "rolled-up" to the protein level according to the Stouffers method for meta-analysis. Our final list of proteins satisfied a q-value of 0.01 as determined by the Benjamini-Hochberg (Reiner et al., 2003) procedure and each had an absolute fold change greater than or equal to 1.5.

Gene Ontology analysis

All Gene Ontology (Carvalho et al., 2009) analyses were carried out using PatternLab's Gene Ontology Explorer module (Carvalho et al., 2016).

Results

We identified 5.719 peptides mapping to 2.400 proteins (1.067 according to the maximum parsimony approach) (Zhang et al., 2007). From the 77 proteins differentially expressed between PCa and BPH tissues (Table 2), after a detailed literature review twenty-one were selected according to their relation with the studied conditions. The selected proteins were: Biglycan (BGN), Calreticulin (CALR), Desmin (DES), Galectin 3 binding protein (LGALS3BP), Galectin-1 (LGALS1), Gelsolin (GSN), Glyceraldehyde-3-phophate dehydrogenase (GAPDH), Heat shock protein family A (Hsp70) member 1A (HSPA1A), Isoform 2 of Transgelin-2 (TAGLN2), kallikrein related peptidase 3 (KLK3), Lactate dehydrogenase A (LDHA), Lactate dehydrogenase B (LDHB), Phosphatidylethanolamine binding protein 1 (PEBP1), Ras suppressor protein 1 (RSU1), S100 calcium binding protein A4 (S100A4), S100 calcium binding protein A6 (S100A6), S100 calcium binding protein A8 (S100A8), S100 calcium binding protein A9 (S100A9), SH3 domain binding glutamate rich protein like (SH3BGRL), Superoxide dismutase 1, soluble (SOD1) and Transgelin (TAGLN).

A gene expression analysis of these 21 preselected showed that only four – the selected ones (Table 3) S100A4, LDHB, PEBP1, RSU1 were statistically significantly in the study.

A gene ontology analysis was used to facilitate the categorization of the identified proteins; pie-charts for each of the Gene Ontology roots are shown in Fig. 1.

The gene interaction network was constructed by associating the four proteins selected involved on the prostate disease (Fig. 2).

This network was generated using STRING database with 0.700 confidence levels. String integrates different curated public databases containing information on direct and indirect functional protein-protein association/interaction (von Mering et al., 2005). Fig. 3 shows the normalized TMT signals from peptides mapping to Phophatidylethanolamine-binding protein 1 RAF (P30086) (protein with higher abundance in PCa) and S100 calcium binding protein A4 (P26447) (protein with lower abundance in PCa).

Table 3
Differentially expressed proteins.

Protein accession	Protein name	Absolut fold change	Sequence count	Spectrum count
P26447	Protein S100-A4	3.91[*]	4	14
P07195	L-lactate dehydrogenase B chain	1.37[*]	8	37
P30086	Phosphatidylethanolamine-binding protein 1 – RAF	1.20[#]	11	51
Q15404	Ras suppressor protein 1	1.46[#]	14	45

[*] Values of BPH when compared with PCa.
[#] Values of PCa when compared with BPH.

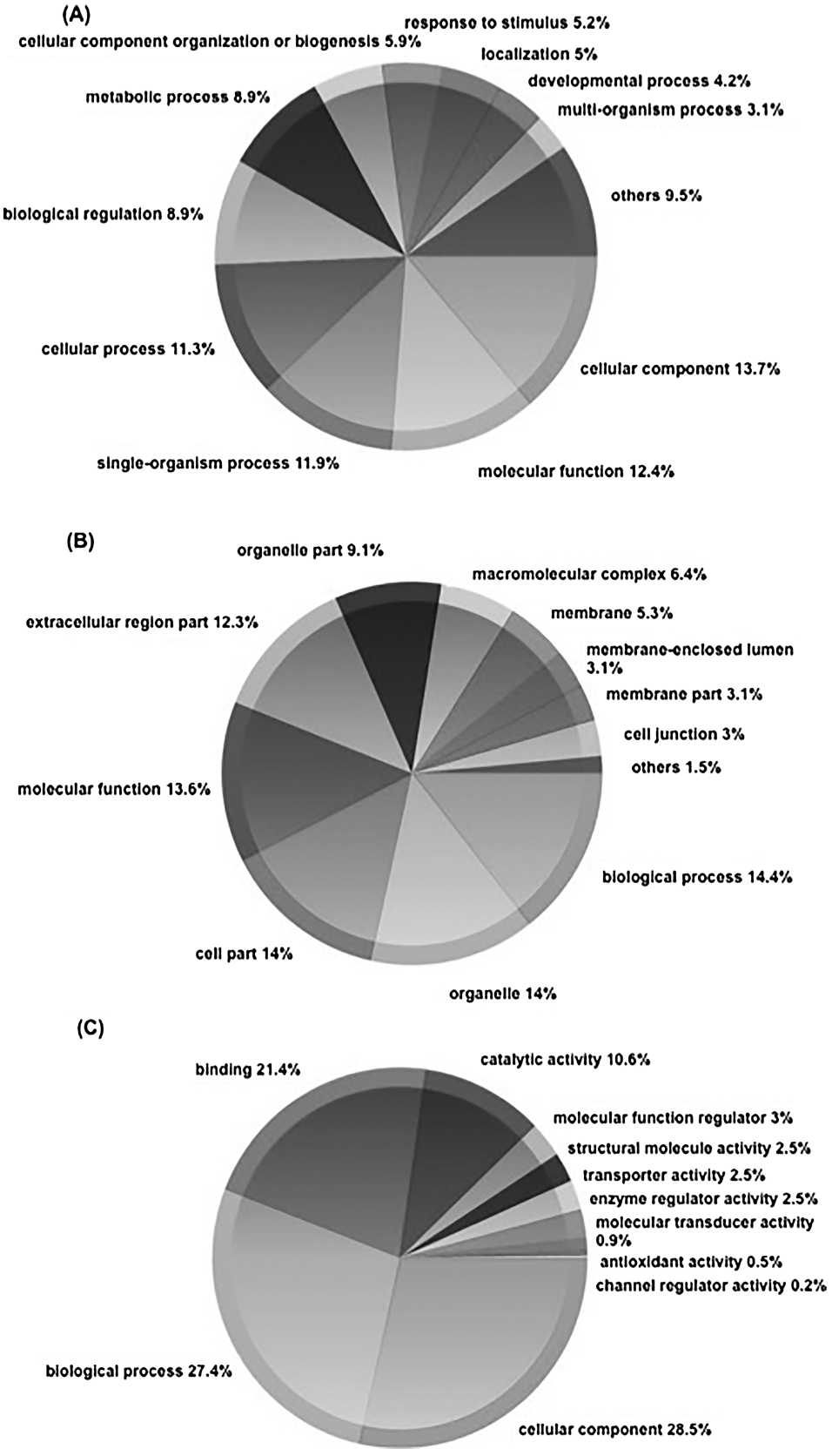

Fig. 1. Functional distribution of the identified proteins in accordance to (A) biological process (B) cellular component (C) molecular function.

The PCa patient group had an average age of 64.33 ± 2.08 years, average PSA serum level of 6.71 ± 0.75 ng/ml and a prostate weight average of 32.33 ± 14.18 g. The BPH group had an average age of 69.67 ± 5.85 years, serum PSA level of 10.24 ± 4.07 ng/ml and a prostate weight of 84.33 ± 45.18 g. The clinical details of the patients are shown in Table 4.

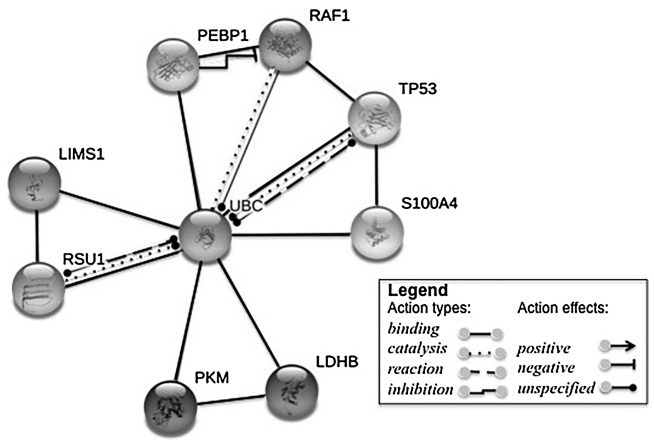

Fig. 2. Protein interaction network from genes RSU1, PEBP1, S100A4 and LDHB evaluated in TaqMan® PCR array.

Among the differentially abundant proteins between BPH and PCa we highlight the proteins that displayed the greatest changes: S100A4, LDHB, RKIP, and Rsu1. S100A4 and LDHB were more abundant in BPH, and this result is in agreement with our q-PCR results. On the other hand, RKIP and Rsu1 were more abundant in PCa samples but showed lower gene expression levels in the q-PCR assay. These results are detailed in Table 5.

Discussion

BPH and PCa present a growing social and clinical burden in an aging population (Lee et al., 2017; Zhou et al., 2016). A reduction in the incidence and progression of such conditions may have formidable economic consequences for national health services (Davalieva et al., 2015a,b). In an effort to better understand the molecular mechanisms responsible for cancer prostate oncogenesis, we sought to identify proteins correlated with this disease. To do this, we compared protein and gene expression in three PCa and three BPH tissue biopsies using quantitative Tandem Mass Tags, and used quantitative real-time PCR to substantiate proteins that were observed to be differentially abundant in the mass spectrometry analysis. Gene Ontology (GO) analysis was used to aid us in interpreting the functions and processes in which the identified proteins are involved.

Ideally, proteomic profiles from healthy prostatic tissue would be included in our study but needless to say, this is hampered by practical and ethical limitations. Instead we compared tissue from malignant prostate tumors and BPH because while cancerous growth of the prostate epithelial cells is characterized by accumulation of molecular abnormalities, BPH represents overgrowth of a more "normal epithelium" with rare genetic abnormalities (De Marzo et al., 1999). This is an established approach for comparing proteomics studies of malignant and benign prostate tissues (Davalieva et al., 2015b; Garbis et al., 2008; Jedinak et al., 2015). An early differential diagnosis between BPH and prostate cancer is essential given the fact that both the outcome and the treatment of these two prostatic diseases are distinct.

Selected proteins showing an upregulation in BPH

S100A4 (metastasin, calvasculin)

The S100 proteins are a multi-gene calcium-binding family comprising 20 known human members each coded by a separate gene. They are characterized by the presence of two Ca^{2+} binding motifs of the EF-hand type interconnected by an intermediate region often referred to as the hinge region (Donato, 2001). Acting as pro inflammatory cytokines, these proteins have been linked with various regulatory functions in acute and chronic

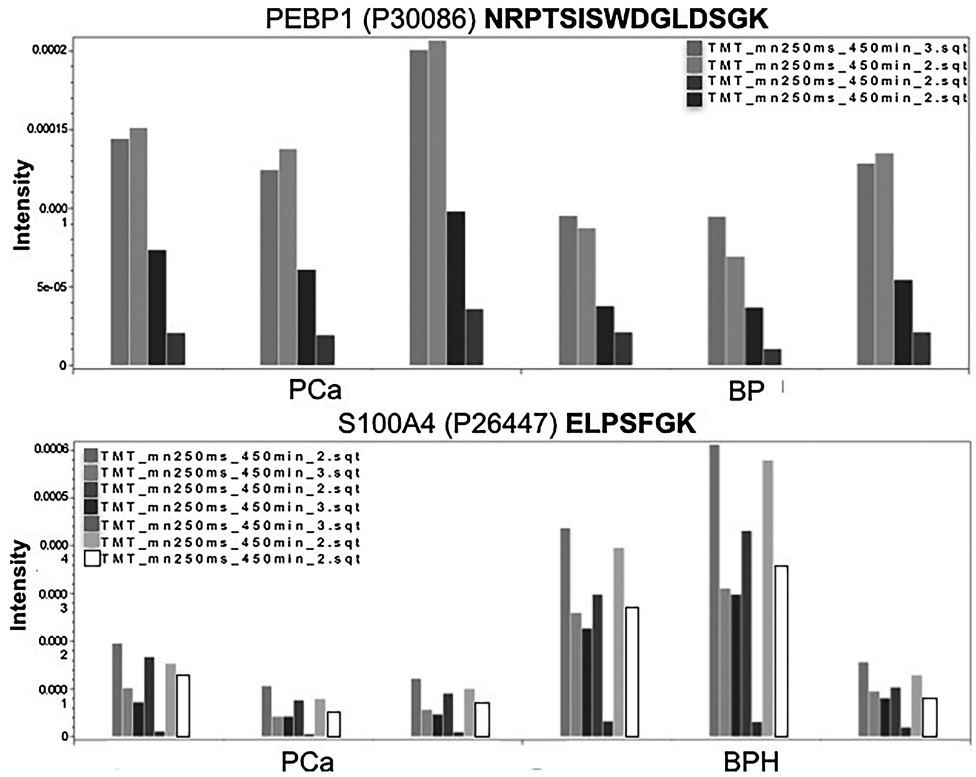

Fig. 3. TMT normalized signals from peptides mapping to S100A4 and to PEBP1. In each plot, each pair of columns with the same color are derived from the same spectrum (markers 126, 127 and 128 corresponding to PCa and 129, 130 and 131 to BPH); this information is necessary for calculating the paired *t*-test.

Table 4
Patient baseline characteristics.

Patient ID	Group	Age (years)	PSA (ng/ml)	Prostate weight (g)	Gleason score
1	PCa	65	5.37	17 g	7 (4 + 3)
2	PCa	66	6.79	45 g	6 (3 + 3)
3	PCa	62	7.98	35 g	7 (4 + 3)
4	BPH	74	14.7	127 g	–
5	BPH	63	9.31	37 g	–
6	BPH	72	6.71	89 g	–

Table 5
Binomial distribution of the genes evaluated for PCa and BPH samples.

Gene	Success for BPH	x (IC 95% – Fisher's)
S100A4	4/4 (100%)	1.0 (0.3976–1.0)
LDHB	4/4 (100%)	1.0 (0.3976–1.0)
PEBP1	4/4 (100%)	1.0 (0.3976–1.0)
RSU1	3/3 (100%)	1.0 (0.2924–1.0)

inflammation (Foell et al., 2007; Oslejskova et al., 2008). It is well known that inflammation is one major factor associated with the development of BPH. Acute and chronic inflammations are implicated in BPH pathogenesis by the increased presence of inflammatory infiltrates and elevated cytokines and chemokines (O'Malley et al., 2014). Recent studies showed S100A4 protein expression is closely associated with the cancer progression, mainly by stimulating cell survival and proliferation, increasing motility and invasion of tumor cells, modifying adhesion of tumor cells (Hou et al., 2018). In contrast, less-differentiated and highly malignant tumor cells present the S100A4 protein in a higher-than-normal abundance and are more sensitive to chemotherapy (Li et al., 2015). Our results corroborate previous findings by showing an overexpression of the *S100A4* gene and a higher abundance of its protein in the BPH samples. However, Gupta et al. demonstrated a moderate to strong expression of S100A4 protein in cancer tissue and increased with tumor aggressiveness based on Gleason grading (Gupta et al., 2003). It is worth noting that we did not evaluate tumors of higher aggressiveness or metastatic patients.

L-lactate dehydrogenase B chain (LDHB)

Lactate dehydrogenase (LDH) is an oxidoreductase enzyme that catalyzes the interconversion of pyruvate and lactate, making it a key glycolytic enzyme. Otto Warburg observed that cancer cells consume much larger quantities of glucose than their normal counterparts and metabolize it predominantly through glycolysis, producing high levels of lactate even in oxygen-rich conditions (Warburg et al., 1927). The inhibition of aerobic glycolysis in cancer cells appears to reduce tumorigenesis, and this has potential to be exploited for anticancer therapies (Chen et al., 2015a). Lactate dehydrogenase is an enzyme composed of LDHA and LDHB. Most of studies showed that LDHA is abundant in many cancers and plays a crucial role in tumor proliferation, invasion, and metastasis, whereas the role of LDHB depends on the type of tumors and remains questionable (Chen et al., 2015a, 2015b; Cui et al., 2015).

Recent studies in pancreatic, hepatocellular, lung squamous cell carcinoma and prostate cancer cells indicate that suppressed expression of the LDHB gene was also due to hypermethylation and that restored expression of LDHB led to decreased LDH activity and lactate production but increased intracellular ATP concentration (Chen et al., 2015b; Cui et al., 2015; Koh et al., 2017; Leiblich et al., 2006). Additionally, Cui et al. (2015) showed that protein levels of LDHB in normal tissues were much higher than in cancer tissues, whereas LDHA was much higher in cancer tissues.

In the current study, we demonstrated lower LDHB gene and protein expression in PCa tissue when compared with BPH. Strategies to restore LDHB expression might be promising for prostate cancer therapeutics and warrant further studies.

Selected proteins showing an upregulation in PCa

Phosphatidylethanolamine-binding protein 1 (PEBP1 or RKIP)

Raf1 kinase inhibitor protein (RKIP) is a member of a conserved group of proteins called phosphatidylethanolamine-binding proteins and regulates multiple important signal pathways including a physiological inhibitor of the Raf-MEK-ERK pathway (Nie et al., 2015).

The Ras-Raf-MEK-ERK/MAPK pathway (MEK is MAPK and ERK kinase, MAPK is mitogen-activated protein kinase, and ERK is extracellular signal-regulated kinase) is an evolutionary conserved pathway that is involved in the control of many fundamental cellular processes that include cell proliferation, survival, differentiation, apoptosis, motility and metabolism. Recent research showed that RKIP not only interferes with the Raf-1-MEK1/2-ERK1/2 signal transduction pathway but also inhibits the signal transduction of NF-κB (nuclear factor Kappa B) and G protein-coupled receptor kinases (Escara-Wilke et al., 2012; Klysik et al., 2008; Wang et al., 2014).

Dysregulation of RKIP expression can potentially be associated with many malignancies (Escara-Wilke et al., 2012; Nie et al., 2015; Yang et al., 2018). Most studies related the lower expression of RKIP with a determinant factor for the metastatic phenotype and progression (Fu et al., 2003; Nie et al., 2015; Yang et al., 2018; Yesilkanal and Rosner, 2014; Zhang et al., 2012). RKIP is initially expressed at a lower level in human metastatic prostate cancer cells than in nonmetastatic cancer cells, and may have a role in preventing vascular invasion of these cells (Fu et al., 2003). Beside this, some studies suggest that activation of the MAP kinase signal transduction pathway is increased as prostate cancer progresses to a more advanced and androgen-independent disease (Fu et al., 2003; Zhang et al., 2012).

Our q-PCR results showed that RKIP is expressed at a lower level in PCa tissues than in BPH, suggesting an association between diminished RKIP expression and the occurrence of tumorigenesis. However, we saw an increase in protein expression of RKIP in PCa samples when compared with BPH tissue, probably from a biological attempt to inhibit MAPK pathway. While these results may seem inconsistent it should be pointed out that mRNA levels do not need to correlate with protein abundancy levels (Bustin et al., 2009).

It has already been demonstrated that RKIP gene expression is negatively correlated with the survival of some types of cells (Yesilkanal and Rosner, 2014; Zhang et al., 2012). Loss or silencing of metastasis suppressor genes plays a key role in modulating key processes involved in cellular growth, EMT, invasion and metastasis (Yang et al., 2018).

We expected to find relatively lower levels of RKIP protein in PCa to correlate with the pathogenesis of disease. Instead, we found higher levels of RKIP protein in PCa samples. It could be that

lower levels of RKIP protein correlate with a metastatic tumor outcome which is not reflective of the patients used in this study. On the other hand, in patients with a non-metastatic disease, the overexpression of this protein could result in a downregulation of the RKIP gene and an inhibition of metastasis and invasiveness.

Ras suppressor protein 1 (Rsu1)

PINCH (cysteine-histidine-rich protein), integrin-linked kinase (ILK) and Ras suppressor-1 (Rsu1) are molecular scaffolding proteins that form a physical complex downstream of integrins, and have overlapping roles in cellular adhesion. Localized at chromosome 10, the Ras suppressor protein 1 (Rsu1) is a leucine rich repeat (LRR) protein that binds to PINCH1 with high affinity *via* its LRR domain. Rsu1 co-localizes with PINCH1 at sites of focal adhesions in mammalian cells and muscle cell attachment in *Drosophila* (Dougherty et al., 2005; Kadrmas et al., 2004; Kim et al., 2015; Tsuda and Cutler, 1993). The inhibition of interaction of these proteins results in decreased cell spreading, cell migration, cell adhesion and reduced motility of mammalian cells (Dougherty et al., 2008; Gonzalez-Nieves et al., 2013; Kim et al., 2015). Some studies have evidenced, *in vitro*, that the inhibition of PINCH1 expression leads to apoptosis in several types of cancers, but *in vivo*, knock out of *Lims1* (which encodes PINCH1) in embryonic neural crest cells caused enhanced apoptosis (Donthamsetty et al., 2013; Dougherty et al., 2008; Liang et al., 2007). Furthermore, the observation that a decrease of Rsu1, but not PINCH1, blocked growth factor induced p38 phosphorylation in MCF10A cells proposed a unique function for Rsu1 (Gonzalez-Nieves et al., 2013). Increasing evidence suggests that the overexpression of Rsu-1 has suppressive proliferation effects on growth of cancer cells (Donthamsetty et al., 2013, Dougherty et al., 2008). Our study demonstrates an increase in the abundance of Rsu1 protein and a decreased expression of the Rsu1 gene in PCa. Taken together, our data support the hypothesis that an upregulation of *Rsu1* gene could increase the protein level in cancer tissue to improve the pro-apoptotic mechanism. Thus, it possibly acts as a control mechanism attempting to stop the initiated metastasis.

Knowing that the oncogenesis of prostate cancer is complex and not completely elucidated, the approach used in this study contributes to our understanding by providing a functional view of the protein and genes networks that could be involved in the oncogenesis process. Previous reports showed only a modest correlation between mRNA and protein levels under a variety of conditions (Schwanhausser et al., 2011; Wu et al., 2013). Since proteins are the functional mediators in phenotype characterization, the study of protein expression profiles in genetically annotated tumors was the inevitable next step.

The application of proteomics in studying the hypothesized precursor lesion should add to our knowledge about the early consequences of prostate disease, which may ultimately lead to early detection biomarkers and potential therapeutic targets. The heterogeneity and the diverse origins of prostate cancer should be more widely embraced in the design of future basic and clinical research studies. Integrative studies are increasingly emerging, creating comprehensive molecular characterizations that can be translated into clinical opportunities (Jedinak et al., 2015; Wu et al., 2013).

Conclusions

Proteomic experiments have contributed significantly to the identification of aberrant proteins and networks, which can serve as targets for biomarker development and individualized therapies. The application of an LC–MS based proteomic method to prostate cancer research was based on the central hypothesis that carcinogenesis involves multiple biological pathways inside the tissue microenvironment and hence requires a more global approach for the discovery of diagnosis/prognosis markers and therapeutic/chemopreventive targets that reflect these pathways. Our findings are a valuable addition to the growing knowledge about the role of these proteins in PCa, providing a starting point for further elucidation of their function in hyperplasia condition and disease initiation. Further studies, including more clinical samples, are needed to unravel the roles of these proteins and genes during the progression and recurrence of PCa.

Conflict of interests

The authors have no conflict of interests to declare.

References

Bayat, A.A., Ghods, R., Shabani, M., Mahmoudi, A.R., Yeganeh, O., Hassannia, H., et al., 2015. Production and characterization of monoclonal antibodies against human prostate specific antigen. Avicenna J. Med. Biotechnol. 7, 2–7.

Bustin, S.A., Benes, V., Garson, J.A., Hellemans, J., Huggett, J., Kubista, M., et al., 2009. The MIQE guidelines: minimum information for publication of quantitative real-time PCR experiments. Clin. Chem. 55, 611–622.

Carvalho, P.C., Fischer, J.S., Chen, E.I., Domont, G.B., Carvalho, M.G., Degrave, W.M., et al., 2009. GO explorer: a gene-ontology tool to aid in the interpretation of shotgun proteomics data. Proteome Sci. 7, 6.

Carvalho, P.C., Lima, D.B., Leprevost, F.V., Santos, M.D., Fischer, J.S., Aquino, P.F., et al., 2016. Integrated analysis of shotgun proteomic data with PatternLab for proteomics 4.0. Nat. Protoc. 11, 102–117.

Charrier, J.P., Tournel, C., Michel, S., Comby, S., Jolivet-Reynaud, C., Passagot, J., et al., 2001. Differential diagnosis of prostate cancer and benign prostate hyperplasia using two-dimensional electrophoresis. Electrophoresis 22, 1861–1866.

Chen, C.Y., Feng, Y., Chen, J.Y., Deng, H., 2015a. Identification of A potent inhibitor targeting human lactate dehydrogenase A and its metabolic modulation for cancer cell line. Bioorg. Med. Chem. Lett. 26, 72–75.

Chen, R., Zhou, X., Yu, Z., Liu, J., Huang, G., 2015b. Low expression of LDHB correlates with unfavorable survival in hepatocellular carcinoma: strobe-compliant article. Med. (Baltim.) 94, e1583.

Cui, J., Quan, M., Jiang, W., Hu, H., Jiao, F., Li, N., et al., 2015. Suppressed expression of LDHB promotes pancreatic cancer progression via inducing glycolytic phenotype. Med. Oncol. 32, 143.

Davalieva, K., Kiprijanovska, S., Komina, S., Petrusevska, G., Zografska, N.C., Polenakovic, M., 2015a. Proteomics analysis of urine reveals acute phase response proteins as candidate diagnostic biomarkers for prostate cancer. Proteome Sci. 13, 2.

Davalieva, K., Kostovska, I.M., Kiprijanovska, S., Markoska, K., Kubelka-Sabit, K., Filipovski, V., et al., 2015b. Proteomics analysis of malignant and benign prostate tissue by 2D DIGE/MS reveals new insights into proteins involved in prostate cancer. Prostate 75, 1586–1600.

De Marzo, A.M., Coffey, D.S., Nelson, W.G., 1999. New concepts in tissue specificity for prostate cancer and benign prostatic hyperplasia. Urology 53, 29–39 discussion 39–42.

Donato, R., 2001. S100: a multigenic family of calcium-modulated proteins of the EF-hand type with intracellular and extracellular functional roles. Int. J. Biochem. Cell. Biol. 33, 637–668.

Donthamsetty, S., Bhave, V.S., Mars, W.M., Bowen, W.C., Orr, A., Haynes, M.M., et al., 2013. Role of PINCH and its partner tumor suppressor Rsu-1 in regulating liver size and tumorigenesis. PLoS One 8, e74625.

Dougherty, G.W., Chopp, T., Qi, S.M., Cutler, M.L., 2005. The Ras suppressor Rsu-1 binds to the LIM 5 domain of the adaptor protein PINCH1 and participates in adhesion-related functions. Exp. Cell. Res. 306, 168–179.

Dougherty, G.W., Jose, C., Gimona, M., Cutler, M.L., 2008. The Rsu-1-PINCH1-ILK complex is regulated by Ras activation in tumor cells. Eur. J. Cell. Biol. 87, 721–734.

Escara-Wilke, J., Yeung, K., Keller, E.T., 2012. Raf kinase inhibitor protein (RKIP) in cancer. Cancer Metastasis Rev. 31, 615–620.

Foell, D., Wittkowski, H., Vogl, T., Roth, J., 2007. S100 proteins expressed in phagocytes: a novel group of damage-associated molecular pattern molecules. J. Leukoc. Biol. 81, 28–37.

Fu, Z., Smith, P.C., Zhang, L., Rubin, M.A., Dunn, R.L., Yao, Z., et al., 2003. Effects of raf kinase inhibitor protein expression on suppression of prostate cancer metastasis. J. Natl. Cancer Inst. 95, 878–889.

Garbis, S.D., Tyritzis, S.I., Roumeliotis, T., Zerefos, P., Giannopoulou, E.G., Vlahou, A., et al., 2008. Search for potential markers for prostate cancer diagnosis, prognosis and treatment in clinical tissue specimens using amine-specific isobaric tagging (iTRAQ) with two-dimensional liquid chromatography and tandem mass spectrometry. J. Proteome Res. 7, 3146–3158.

Gleason, D.F., 1992. Histologic grading of prostate cancer: a perspective. Hum. Pathol. 23, 273–279.

Gonzalez-Nieves, R., Desantis, A.I., Cutler, M.L., 2013. Rsu1 contributes to regulation of cell adhesion and spreading by PINCH1-dependent and – independent mechanisms. J. Cell. Commun. Signal. 7, 279–293.

Gupta, S., Hussain, T., Maclennan, G.T., Fu, P., Patel, J., Mukhtar, H., 2003. Differential expression of S100A2 and S100A4 during progression of human prostate adenocarcinoma. J. Clin. Oncol. 21, 106–112.
Hou, S., Tian, T., Qi, D., Sun, K., Yuan, Q., Wang, Z., et al., 2018. S100A4 promotes lung tumor development through beta-catenin pathway-mediated autophagy inhibition. Cell. Death Dis. 9, 277.
Jedinak, A., Curatolo, A., Zurakowski, D., Dollon, S., Bhasin, M.K., Libermann, T.A., et al., 2015. Novel non-invasive biomarkers that distinguish between benign prostate hyperplasia and prostate cancer. BMC Cancer 15, 259.
Jemal, A., Center, M.M., Desantis, C., Ward, E.M., 2010. Global patterns of cancer incidence and mortality rates and trends. Cancer Epidemiol. Biomarkers Prev. 19, 1893–1907.
Kadrmas, J.L., Smith, M.A., Clark, K.A., Pronovost, S.M., Muster, N., Yates 3rd, J.R., Beckerle, M.C., 2004. The integrin effector PINCH regulates JNK activity and epithelial migration in concert with Ras suppressor 1. J. Cell. Biol. 167, 1019–1024.
Kim, Y.C., Gonzalez-Nieves, R., Cutler, M.L., 2015. Rsu1 contributes to cell adhesion and spreading in MCF10A cells via effects on P38 map kinase signaling. Cell. Adh. Migr. 9, 227–232.
Klysik, J., Theroux, S.J., Sedivy, J.M., Moffit, J.S., Boekelheide, K., 2008. Signaling crossroads: the function of Raf kinase inhibitory protein in cancer, the central nervous system and reproduction. Cell. Signal. 20, 1–9.
Koh, Y.W., Lee, S.J., Park, S.Y., 2017. Prognostic significance of lactate dehydrogenase B according to histologic type of non-small-cell lung cancer and its association with serum lactate dehydrogenase. Pathol. Res. Pract. 213, 1134–1138.
Kozal, S., Peyronnet, B., Cattarino, S., Seisen, T., Comperat, E., Vaessen, C., et al., 2015. Influence of pathological factors on oncological outcomes after robot-assisted radical prostatectomy for localized prostate cancer: results of a prospective study. Urol. Oncol. 33 (330), e1–e7.
Lee, S.W.H., Chan, E.M.C., Lai, Y.K., 2017. The global burden of lower urinary tract symptoms suggestive of benign prostatic hyperplasia: a systematic review and meta-analysis. Sci. Rep. 7, 7984.
Leiblich, A., Cross, S.S., Catto, J.W., Phillips, J.T., Leung, H.Y., Hamdy, F.C., et al., 2006. Lactate dehydrogenase-B is silenced by promoter hypermethylation in human prostate cancer. Oncogene 25, 2953–2960.
Li, W.L., Zhang, Y., Liu, B.G., Du, Q., Zhou, C.X., Tian, X.S., 2015. Correlation between the expression of S100A4 and the efficacy of TAC neoadjuvant chemotherapy in breast cancer. Exp. Ther. Med. 10, 1983–1989.
Liang, X., Sun, Y., Schneider, J., Ding, J.H., Cheng, H., Ye, M., et al., 2007. Pinch1 is required for normal development of cranial and cardiac neural crest-derived structures. Circ. Res. 100, 527–535.
Mazzucchelli, R., Colanzi, P., Pomante, R., Muzzonigro, G., Montironi, R., 2000. Prostate tissue and serum markers. Adv. Clin. Path. 4, 111–120.
McAlister, G.C., Nusinow, D.P., Jedrychowski, M.P., Wuhr, M., Huttlin, E.L., Erickson, B.K., et al., 2014. MultiNotch MS3 enables accurate, sensitive, and multiplexed detection of differential expression across cancer cell line proteomes. Anal. Chem. 86, 7150–7158.
Nie, F., Cao, J., Tong, J., Zhu, M., Gao, Y., Ran, Z., 2015. Role of Raf-kinase inhibitor protein in colorectal cancer and its regulation by hydroxycamptothecine. J. Biomed. Sci. 22, 56.
O'Malley, K.J., Eisermann, K., Pascal, L.E., Parwani, A.V., Majima, T., Graham, L., et al., 2014. Proteomic analysis of patient tissue reveals PSA protein in the stroma of benign prostatic hyperplasia. Prostate 74, 892–900.
Oslejskova, L., Grigorian, M., Gay, S., Neidhart, M., Senolt, L., 2008. The metastasis associated protein S100A4: a potential novel link to inflammation and consequent aggressive behaviour of rheumatoid arthritis synovial fibroblasts. Ann. Rheum. Dis. 67, 1499–1504.
Pin, E., Fredolini, C., Petricoin 3rd, E.F., 2013. The role of proteomics in prostate cancer research: biomarker discovery and validation. Clin. Biochem. 46, 524–538.
Reiner, A., Yekutieli, D., Benjamini, Y., 2003. Identifying differentially expressed genes using false discovery rate controlling procedures. Bioinformatics 19, 368–375.
Schwanhausser, B., Busse, D., Li, N., Dittmar, G., Schuchhardt, J., Wolf, J., et al., 2011. Global quantification of mammalian gene expression control. Nature 473, 337–342.
Siegel, R.L., Miller, K.D., Jemal, A., 2018. Cancer statistics, 2018. CA Cancer J. Clin. 68, 7–30.
Thompson, A., Schafer, J., Kuhn, K., Kienle, S., Schwarz, J., Schmidt, G., et al., 2003. Tandem mass tags: a novel quantification strategy for comparative analysis of complex protein mixtures by MS/MS. Anal. Chem. 75, 1895–1904.
Tsuda, T., Cutler, M.L., 1993. Human Rsu1 is highly homologous to mouse Rsu-1 and localizes to human chromosome 10. Genomics 18, 461–462.
von Mering, C., Jensen, L.J., Snel, B., Hooper, S.D., Krupp, M., Foglierini, M., et al., 2005. STRING: known and predicted protein-protein associations, integrated and transferred across organisms. Nucleic Acids Res. 33, D433–D437.
Wang, Q., Wu, X., Wu, T., Li, G.M., Shi, Y., 2014. Clinical significance of RKIP mRNA expression in non-small cell lung cancer. Tumour Biol. 35, 4377–4380.
Warburg, O., Wind, F., Negelein, E., 1927. The metabolism of tumors in the body. J. Gen. Physiol. 8, 519–530.
Washburn, M.P., Wolters, D., Yates 3rd, J.R., 2001. Large-scale analysis of the yeast proteome by multidimensional protein identification technology. Nat. Biotechnol. 19, 242–247.
Whitfield, E.J., Pruess, M., Apweiler, R., 2006. Bioinformatics database infrastructure for biotechnology research. J. Biotechnol. 124, 629–639.
Wu, L., Candille, S.I., Choi, Y., Xie, D., Jiang, L., Li-Pook-Than, J., et al., 2013. Variation and genetic control of protein abundance in humans. Nature 499, 79–82.
Yang, K., Li, Y., Lian, G., Lin, H., Shang, C., Zeng, L., et al., 2018. KRAS promotes tumor metastasis and chemoresistance by repressing RKIP via the MAPK-ERK pathway in pancreatic cancer. Int. J. Cancer 142, 2323–2334.
Yesilkanal, A.E., Rosner, M.R., 2014. Raf kinase inhibitory protein (RKIP) as a metastasis suppressor: regulation of signaling networks in cancer. Crit. Rev. Oncog. 19, 447–454.
Zeidan, B.A., Townsend, P.A., Garbis, S.D., Copson, E., Cutress, R.I., 2015. Clinical proteomics and breast cancer. Surgeon 13, 271–278.
Zhang, B., Chambers, M.C., Tabb, D.L., 2007. Proteomic parsimony through bipartite graph analysis improves accuracy and transparency. J. Proteome Res. 6, 3549–3557.
Zhang, H., Wu, J., Keller, J.M., Yeung, K., Keller, E.T., Fu, Z., 2012. Transcriptional regulation of RKIP expression by androgen in prostate cells. Cell. Physiol. Biochem. 30, 1340–1350.
Zhou, C.K., Check, D.P., Lortet-Tieulent, J., Laversanne, M., Jemal, A., Ferlay, J., et al., 2016. Prostate cancer incidence in 43 populations worldwide: an analysis of time trends overall and by age group. Int. J. Cancer 138, 1388–1400.